ARL-CR-0815 ● JUNE 2017

US Army Research Laboratory

Progress toward Topology Optimization (TO) for Additive Manufacturing (AM) and Fatigue

prepared by Terrence E Johnson
Oak Ridge Associated Universities (ORAU)
4692 Millennium Drive, Suite 101
Belcamp, MD 21017

under contract W911NF-16-2-0093

NOTICES

Disclaimers

The findings in this report are not to be construed as an official Department of the Army position unless so designated by other authorized documents.

Citation of manufacturer's or trade names does not constitute an official endorsement or approval of the use thereof.

Destroy this report when it is no longer needed. Do not return it to the originator.

ARL-CR-0815 ● JUNE 2017

US Army Research Laboratory

Progress toward Topology Optimization (TO) for Additive Manufacturing (AM) and Fatigue

prepared by Terrence E Johnson
Oak Ridge Associated Universities (ORAU)
4692 Millennium Drive, Suite 101
Belcamp, MD 21017

under contract W911NF-16-2-0093

REPORT DOCUMENTATION PAGE

Form Approved
OMB No. 0704-0188

1. REPORT DATE *(DD-MM-YYYY)*	2. REPORT TYPE	3. DATES COVERED (From - To)
June 2017	Contractor Report	May 2015–May 2017

4. TITLE AND SUBTITLE
Progress toward Topology Optimization (TO) for Additive Manufacturing (AM) and Fatigue

5a. CONTRACT NUMBER
W911NF-16-2-0093

5b. GRANT NUMBER

5c. PROGRAM ELEMENT NUMBER

6. AUTHOR(S)
Terrence E Johnson

5d. PROJECT NUMBER

5e. TASK NUMBER

5f. WORK UNIT NUMBER

7. PERFORMING ORGANIZATION NAME(S) AND ADDRESS(ES)
Oak Ridge Associated Universities (ORAU)
4692 Millennium Drive, Suite 101
Belcamp, MD 21017

8. PERFORMING ORGANIZATION REPORT NUMBER
ARL-CR-0815

9. SPONSORING/MONITORING AGENCY NAME(S) AND ADDRESS(ES)
US Army Research Laboratory
Vehicle Technology Directorate ATTN: VTD-TVM
Aberdeen Proving Ground, MD 21005-5066

10. SPONSOR/MONITOR'S ACRONYM(S)

11. SPONSOR/MONITOR'S REPORT NUMBER(S)

12. DISTRIBUTION/AVAILABILITY STATEMENT
Approved for public release; distribution is unlimited.

13. SUPPLEMENTARY NOTES

14. ABSTRACT

This report summarizes research progress to date in topology optimization (TO) for additive manufacturing (AM) and fatigue. The effort has been divided into 2 parts: TO for AM and TO for fatigue of metals. The 2-D and 3-D solutions are presented for TO for AM and fatigue. The proposed design approaches have produced promising results and suggest further investigation. A path forward is suggested in the conclusion.

15. SUBJECT TERMS
topology optimization, fatigue, additive manufacturing, TO, AM

16. SECURITY CLASSIFICATION OF:			17. LIMITATION OF ABSTRACT	18. NUMBER OF PAGES	19a. NAME OF RESPONSIBLE PERSON
a. REPORT	b. ABSTRACT	c. THIS PAGE			Terrence E Johnson
Unclassified	Unclassified	Unclassified	UU	28	19b. TELEPHONE NUMBER (Include area code) 410-278-1749

Contents

List of Figures

List of Tables

Acknowledgments

The Topology Optimization (TO) for Additive Manufacturing (AM) work was done in collaboration with Dr Andy Gaynor of the US Army Research Laboratory's Weapons and Materials Research Directorate. Andy used his TO code to produce the solutions shown in Figs. 3, 5, and 9–12.

INTENTIONALLY LEFT BLANK.

1. Introduction

Additive manufacturing (AM) is a layer-by-layer manufacturing method that builds parts from the bottom up. This way of manufacturing is relatively new, first appearing in the 1980s. AM is different from the traditional subtractive manufacturing process, which cuts away material from a starting substrate to get a final component. Topology optimization (TO) is an extremely powerful free-form rigorous design method that was developed for designing structures. TO can produce efficient designs for prescribed objectives and constraints that make it ideal for AM. AM has the capacity to realize TO designs that are not realizable by traditional manufacturing processes due to cost, tool-path constraints, or operator limitations. While AM significantly widens the design space for TO, manufacturing constraints and limitations remain[1] and should be addressed in the design process. An objective of this work is to consider manufacturing constraints, such as overhangs and enclosed pores, within the TO methodology for structural design.

Fatigue is a fundamental mode of failure in vibrating structures such as rotorcraft. Current US Army rotorcraft maintenance schedules are costly as they can keep aircraft grounded for an extended time period and require manual labor to survey the structure for possible damage caused by fatigue. Structures with improved fatigue properties could therefore reduce maintenance costs. Traditional TO formulations for lightweighting (i.e., without consideration of fatigue) often produce designs with stress concentrations or singularities that cause a reduction in fatigue life. Manual adjustments or additional structural optimization are needed to fulfill engineering stress requirements. Therefore, a second objective of this work is to consider/couple fatigue within TO design for the lightweighting of structures.

This report presents progress that has been made toward designing lightweight, fatigue-constrained topologically optimized structures using AM. To date, this research effort has been divided into 2 distinct components: 1) TO for AM, 2) TO for fatigue. Future plans call for these component algorithms to be combined and demonstrated as TO for AM and fatigue.

The goal of TO for AM is to design structures that account for AM limitations within the design. The limitations of interest in this work are the production of support material and enclosed pores. Both limitations will be separately considered in the TO formulation.

The goal of TO for fatigue is to codify and experimentally demonstrate a TO-capability to maintain or enhance fatigue life. This will be done by selecting a published methodology for handling stress within TO and use it to develop 3-D TO

solutions. The solutions will be realized/proven/demonstrated using traditional manufacturing techniques and fatigue-testing protocols. Though a non-AM process will be used here, the novelty of this second effort is fatigue testing of a TO-designed structure. This work will verify the selected stress handling methodology and produce test results that will serve as a benchmark for TO for stress and fatigue efforts.

This report is outlined as follows: Section 2 gives an overview of the overhang and void-projection schemes used to account for AM constraints. Section 3 describes the TO problem formulation that is used to generate solutions for the presented projection schemes. Section 4 presents the solution to the problem formulation given in Section 3. Section 5 presents the approach selected for accounting for stress within a TO structure. Section 6 presents the TO problem formulation used to demonstrate the methodology presented in Section 5. Section 7 presents examples that solve the TO problem formulation given in Section 6. The report ends with a summary and concluding remarks in Sections 8 and 9.

2. Overhang Projection and Void Projection

An overhang is a solid feature that rises in the build direction, at a shallow angle to horizontal, with supporting material below it. In extrusion-based processes, support material is generated during fabrication to hold-up soft overhang material as it hardens to prevent part distortion. Following fabrication, support material removal can result in surface damage, trapped material, increased part time and fabrication cost. In metal powder bed fusion processes, support material is generated during fabrication to prevent solid feature distortion from residual stress accumulation because of thermal gradients within the sintered solid and to produce a conductive path from the point of melting/sintering to the build plate. Following fabrication, support material removal can lead to degraded surface finish, trapped material, increased part time, and fabrication cost. Therefore, several research efforts aim to remove overhangs from designed structures.[1–11] In this work, overhangs are removed by making structures self-supporting.

The proposed approach to make a structure self-supporting is to account for overhangs in the TO design formulation. The proposed method is 3-D and an extension of work done by Gaynor and Guest.[6] In that work, overhangs were totally eliminated by a so-called overhang projection scheme. The idea behind the overhang projection scheme is simple: an element (e) may become a solid element if and only if the following occur: 1) the local design variables indicate material should be deposited into the element[12] and 2) sufficient material exists in the supporting elements below e such that e does not violate the defined overhang

angle. If *e* becomes solid, it will not contribute to an overhang. Three variables are used to create this effect: 1) the φ is the vector of dependent variables that is passed through the Heaviside Projection Method (HPM) to create a spherical[6] solid feature in the finite element space, 2) the ψ is the vector of independent design variables that indicates whether material should be deposited at a given location, and 3) the ρ_S is a subset of variables φ that exist in the neighborhood below the point of interest (Fig. 1) and indicate whether material can be deposited at the considered location (i.e., indicate whether or not the overhang condition is violated). The Ψ and ρ_S will be combined to form φ, which is then used to determine element volume fraction ρ^e: $\varphi^j = \Psi^i * \rho_S{}^i$. Whether material can be projected from a point φ^i onto the elemental domain is entirely dependent on the magnitudes of other φ variables below this point, and thus the algorithm must proceed in a layer-by-layer manner, essentially mimicking actual AM processes. The overhang support neighborhood that relates a given Ψ^i to the support region below it is shown in Fig. 1. In Fig. 1, the blue dots represent locations within the finite element domain that have an assigned variable Ψ^i. The green dots represent locations below Point *i* that represent the neighborhood where ρ_S is calculated. The Ψ and ρ_S determine if material should be placed at Point *i*.

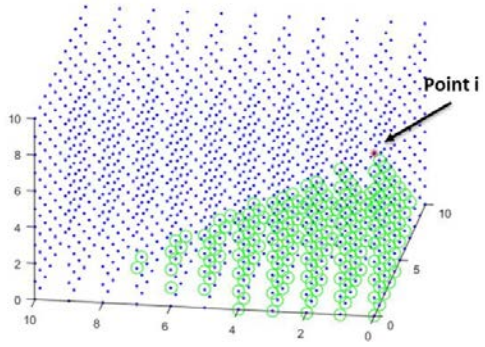

Fig. 1 3-D search design domain

The density of an element is defined by Eq. 1. If $\rho^e = 1$, then the element is solid. If $\rho^e = 0$, then the element is void. The β is the regularization parameter dictating the aggressiveness of the regularized Heaviside function.[12] The μ^e is the proximity weighted-average of design variables defined by φs in a spherical neighborhood with a prescribed radius (r_{min}) from an element of interest *e*. The φ_{max} is the maximum magnitude of φ (herein = to 1).

$$\rho^e = 1 - e^{-\beta\mu^e(\varphi)} + \frac{\mu^e(\varphi)}{\varphi_{max}} e^{-\beta\varphi_{max}} \quad (1)$$

To recap, the elemental densities ρ^e are computed by Eq. 1 and are a function of dependent variable φ^j. The φ^j is a function of the independent optimization variable Ψ^i and the dependent support indicator variable $\rho_S{}^i$. The $\rho_S{}^i$ is computed using a

relationship given in Gaynor and Guest[6] and are a function of φ in the support neighborhood below the considered point, *i*. This last dependency means that the algorithm must proceed in a layer-by-layer manner starting from the bottom.

Lastly, this underlying algorithm may be slightly adjusted to solve a completely different problem in TO for AM: the enclosed pore solution. Enclosed pores are hollow sections of a volume, which should be filled only with air. However, in metal powder bed fusion processes, these hollow sections will trap powder that is very difficult (if not impossible) to remove without severely damaging the structure. This may also be an issue in extrusion-based processes where support material can get trapped. This work proposes a simple approach to removing enclosed pores in TO design: void projection. Void projection can be accomplished in TO using Eq. 2:

$$\rho^e = -e^{-\beta\mu^e(\varphi)} + \frac{\mu^e(\varphi)}{\varphi_{max}} e^{-\beta\varphi_{max}} . \tag{2}$$

The idea being that instead of projecting solid material from the design variables (which are located at the nodes), the algorithm project voids. When this is coupled to the layer-by-layer bottom-up approach discussed for overhang projections, the result is structures with void pathways that ensure material removal. This is further discussed in Section 4.2.

3. Problem Formulation (TO for AM)

The proposed scheme for TO for AM is demonstrated using the well-known[13] minimum compliance (maximum stiffness) problem. The goal of the optimization will be to simultaneously satisfy the objective function and constraints while searching for the location within the design space where the gradient of the objective function is zero. The location within the designs space where the gradient is zero can be a local or global minimum or maximum to the objective function. To achieve its goal, the optimization process determines the material distribution, ρ^e, of the elements within the design domain. The optimization formulation takes on the following form:

$$\begin{cases} \min \boldsymbol{F}^T\boldsymbol{d} \\ s.t. \begin{cases} \boldsymbol{K}\boldsymbol{d} = \boldsymbol{F}, \\ \sum \rho^e v^e \leq V \end{cases} \end{cases} , \tag{3}$$

where $\boldsymbol{F}^T\boldsymbol{d}$ (compliance) is the objective function, $\boldsymbol{K}\boldsymbol{d} = \boldsymbol{F}$ (equilibrium), and $\sum \rho^e v^e \leq V$ is the volume constraint.

$\boldsymbol{F}$ is the vector of applied nodal loads, $\boldsymbol{d}$ is the vector of nodal displacements, $\boldsymbol{K(\psi)}$ is the global stiffness matrix, $\rho^e(\boldsymbol{\psi})$ is elemental volume fraction of element *e*, v^e is

the volume of element *e* and *V* is the total allowable material volume. The Ψ^i varies between 0 and 1. The element density ρ^e affects structural equilibrium through the global stiffness matrix. The global stiffness definitions of interest in this work are RAMP and SIMP and RAMP defined in Eqs. 4 and 5, respectively[13–15]:

$$\boldsymbol{K}^e = \left(\rho_{min} + \frac{\rho^e}{1+\gamma(1-\rho^e)}\right)\boldsymbol{K}_0^e \tag{4}$$

$$\boldsymbol{K}^e = \left(\rho_{min} + \rho^{e\gamma}\right)\boldsymbol{K}_0^e\,. \tag{5}$$

Both produce quality solutions, yet a preference has been developed for RAMP because of its nonzero gradient at $\rho^e = 0$. This property was useful as material grew out of void space below a structural feature to make said feature self-supporting. Similar benefits are seen in Guest[16] where it was necessary for stiff inclusions to grow out of compliant matrix material.

4. Examples (TO for AM)

The proposed methodologies for overhang and void projection are demonstrated using simple 2-D and 3-D structures described in Sections 4.1 and 4.2. The radial length scale (r_{min}) prescribed in the 3-D overhang projection examples is 2 times the element length. The allowable volume fraction is 50% and the initial distribution of ψ is a uniform 50%. The SIMP exponent 5 is chosen to further make densities that are less than 1 inefficient by reducing their stiffness value. The β used in the density definition is 25. Selecting a value of 25 further increases the algorithm's ability to eliminate intermediate density elements at the structure's boundary. In all examples, the optimization process was run for several iterations until convergence was obtained.

4.1 Overhang Projection

The first example used to demonstrate the proposed 3-D solid projection self-supporting scheme is the 3-D cantilever beam (Fig. 2). The mesh is composed of 4-node brick elements that are 1:1:1 in aspect ratio. The angular self-support condition is 45° from horizontal. The solution (Fig. 3) shows that the imposed angular restriction of 45° has not been exceeded. This fundamentally demonstrates that the optimization process can build structures from the bottom up without violating the imposed constraint on the feature angle. The cliff that exist at the right-most edge is needed to support the external load. The removed sections of the beam beneath the cliff and in the interiors result from the optimization process working to satisfy the volume fraction constraint of 50% and minimize compliance. Constraining the volume of the final solution is effectively how the optimization

process lightweights the structure. The obtained solution is a local minimum in a nonconvex design space.

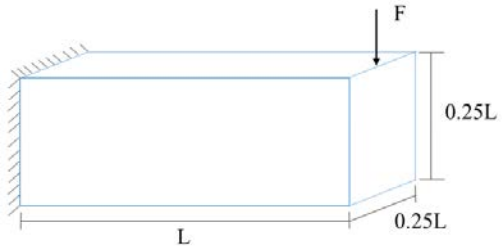

Fig. 2 3-D cantilever beam

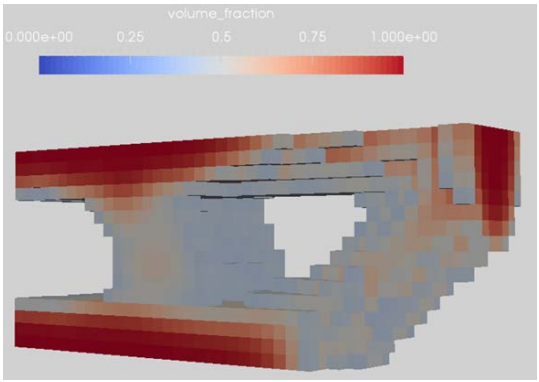

Fig. 3 TO solution for 3-D cantilever beam

The second example is a 3-D tall rectangular box that sits on a base (Fig. 4). The base represents the base plate in an AM machine—such as a Stratasys FDM printer. The printing direction is in the vertical direction from the base plate. This example is intended to show that the algorithm actively works to ensure that the structure is self-supporting by building the structure from the baseplate. It can be seen (Fig. 5) that no part of the structure has angular features less than 45°. The solution is multicolored, which means it is not physically realizable. A physically realizable solution would be an all-solid color (e.g., all red). Thus, interpretive work must be done by the designer to realize the solution (through thresholding out low-density elements, thus defining the solid structure by those finite elements above the threshold).

Fig. 4 3-D Column with AM base plate

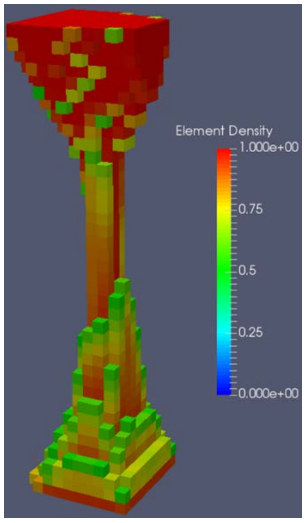

Fig. 5 Solution of 3-D column with AM base plate

4.2 Void Projection

The void projection scheme is demonstrated using 2-D (Figs. 6 and 7) and 3-D beam (Fig. 8) problems. In 2-D, the elements are 4-node quadrilaterals that have an aspect ratio of 1:1. The rim in the 2-D void projection example is 2 times the element length. The beam in Fig. 6 represents half of a Messerschmidt-Bolkow-Blohm (MBB) beam. Since the load, geometry, and boundary conditions (3-point bending) are symmetric about the center of the beam, only half of the beam needs to be topologically optimized. The half solution can then be mirrored about the vertical line of symmetry of the beam. The half beam is used in solving the problem.

The solution in Fig. 9 shows a full beam with a cutout section. Blue represents void (no material). Red represents solid (material). The cutout section defined by the optimization process is beneath the solid section because the void projection scheme will always opt to remove material from the bottom up unless doing so will violate the design constraints or equilibrium. The resulting physical topology is one that does not trap material. This is also seen in the topologically optimized solutions in Figs. 10–12.

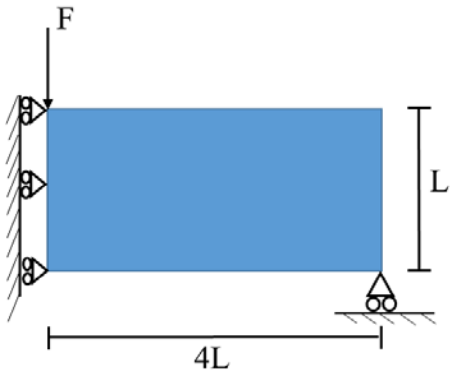

Fig. 6 2-D simply supported beam definition

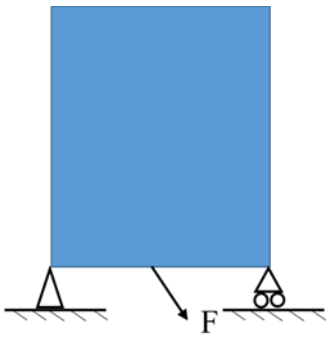

Fig. 7 2-D short beam definition

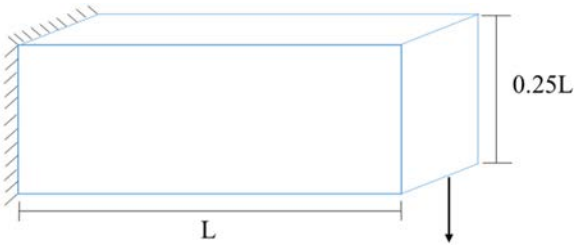

Fig. 8 3-D cantilever beam definition

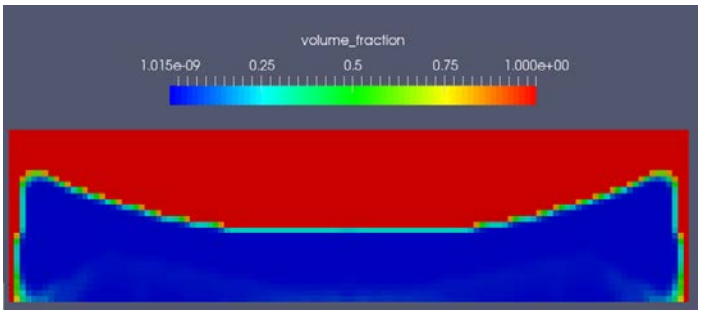

Fig. 9 Solution for simply supported beam in Fig. 6

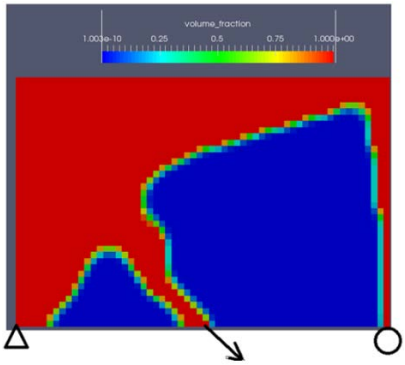

Fig. 10 Solution to short beam in Fig. 7

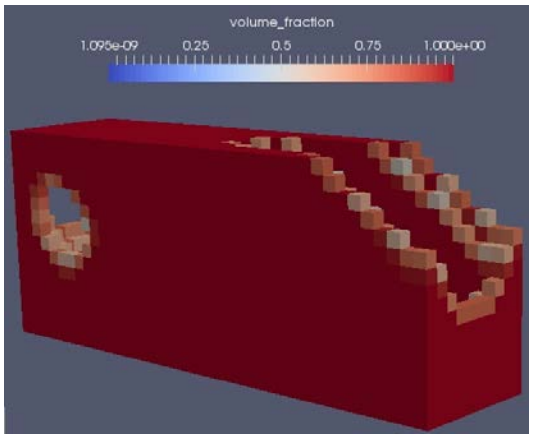

Fig. 11 Solution to cantilever beam in Fig. 8

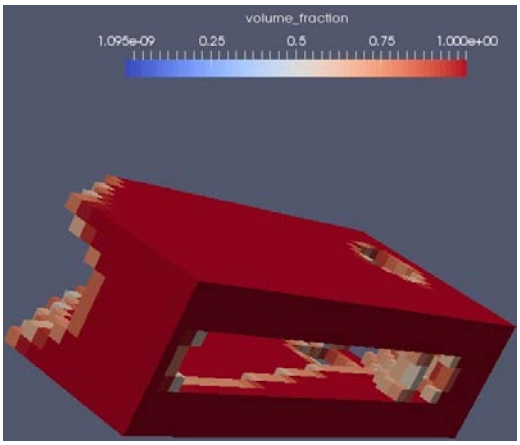

Fig. 12 Reorientation of solution in Fig. 11

The short beam problem (Fig. 7) has a slanted load and is intended to demonstrate how the optimization process adjusts for load orientation. The solution in Fig. 10 is particularly interesting because a feature is extruded from the bulk solid section to support a slanted load (see Fig. 7 for the initial geometry and problem setup). The optimization process is formulated to remove at least 50% of the material from the bottom up and does so as seen in the large blue region. The remaining solid section is used for directing the load to the boundaries.

In 3-D (Fig. 11), the same phenomenon is seen: the optimization process removes material from the bottom up to satisfy the volume constraint. The prescribed volume constraint is 50%. Solid material is removed from sections that have less impact on the load path from the load to the cantilever boundary conditions. Figure 11 shows a hole in the beam near the boundary. Figure 12 shows that the hole extends through to beam's cross section. This hole is a discontinuity in the beam and therefore causes stress concentrations. This denotes the need to introduce stress constraints within the optimization process. Overall, the 2-D and 3-D examples show that the proposed void projection scheme produces solutions that are not likely to trap material.

5. Clustered Fatigue Stress Measure and Stress Life Calculation (TO for Fatigue)

Fatigue life can be enhanced or maintained while lightweighting by accounting for stress. That is, there is a direct correlation between stress reduction and prolonged fatigue life. As a result, the handling of stress is of primary importance. Within a finite-based TO realm, stress can be handled locally, globally, or in clusters. The approach of interest in this work is the clustered approach proposed by Holmberg et al.[17] Clusters are groupings of stress from elements in the FE domain. The

number of groups can vary from 1 (i.e., globally: all elemental stresses are grouped into 1 set) to the maximum number of stresses calculated from the finite element system (i.e., locally: there is 1 cluster per integration point). The clustered stress definition is as follows:

$$\sigma_i^{PN} = \left(\frac{1}{N_i}\sum_{a\in\omega_i}\left(\sigma_a^{vM}(\boldsymbol{x})\right)^p\right)^{\frac{1}{p}}. \tag{6}$$

The von Mises stress measure, σ_a^{vM}, is calculated at an integrate point within a finite element. The N_i is the number of stress points considered in a cluster. It acts as a built-in scaling of σ_i^{PN}, which is beneficial for convergence in optimization problems. The p is called the *p-Norm* exponent and is set equal to 8.[17] Von Mises is a function of σ_a given in Eq. 7. The σ_a is a function of penalization factor δ_s, which is used to increase the stress values of element with intermediate density, thereby making them inefficient and candidates for elimination from the final design domain. The optimal final density distribution within the design domain is 0–1. Intermediate densities require further analysis and interpretation by the designer.

$$\sigma_a(\boldsymbol{x}) = \delta_s(\rho_e(\boldsymbol{x}))\hat{\sigma}_a(\boldsymbol{x}) \tag{7}$$

6. Problem Formulation (TO for Fatigue)

The optimization problem formulation used to demonstrate fatigue life enhancement and preservation is handled using stress constraints. The formulation is as follows:

$$\begin{cases} \min\limits_{x} \sum m_e\rho_e(\boldsymbol{x}) \\ s.t. \begin{cases} \sigma_i^{PN}(\boldsymbol{x}) \le \bar{\sigma},\ i = 1,\dots,n_c \\ \underline{x_e} \le x_e \le \overline{x_e},\ e = 1,\dots,n_e \end{cases} \end{cases}, \tag{8}$$

where n_e is the number of design variables and m_e is the solid element mass related to design variable e. The *e:th* variable[8] is denoted ρ_e ($\boldsymbol{x}$) and x_e is the *e:th* design variable, limited by the box constraint limits $x_e = 1$ and $x_e = e$, where e is a small positive number used to avoid the stiffness matrix becoming singular. The stress measure is the modified *P-norm* based on von Mises stresses, which for cluster number i is denoted $\sigma_i^{PN}(\boldsymbol{x})$. The number of clusters, or equally, the number of stress constraints, is denoted n_c and $\bar{\sigma}$ is the stress limit. In the previous formulation, the equilibrium equation is not used as a constraint. Instead, the displacement vector results from the calculation of $u=K^{-1}(x)\ F$ within the algorithm (i.e., nested formulation). The stiffness penalization is SIMP as described previously in Section 4.

7. Examples (TO for Fatigue)

The examples used to demonstrate Holmberg's stress constraint formulation are the cantilever with shear load and the MMB beam. The elements used in the finite element domain are 2-D plane elements. The element type is 4-node quadrilaterals. The number of elements in the initial design domain is 300 (10 × 30). The solutions were run to 500 iterations. The topologically optimized solutions in Figs. 14 and 17 show the density distributions.

7.1 Cantilever in Shear

The design domain for the problem is given in Fig. 13. The density and stress distributions are given in Figs. 14 and 15. The external load is distributed over several nodes to relieve stress concentrations that result from applying point loads. The initial distribution of φ is uniform at 2%. The optimization algorithm used to solve this problem is Matlab's[18] "fmincon". The derivatives were provided to fmincon following the formulation in Holmberg.[17] The Heaviside projection[12] method was used to calculate density.

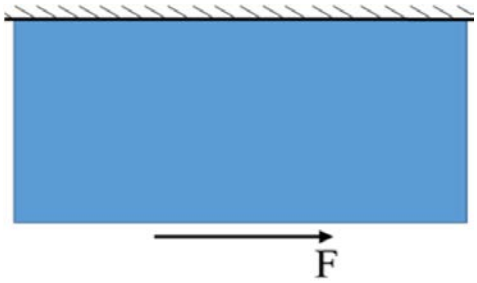

Fig. 13 Initial geometry for shear problem

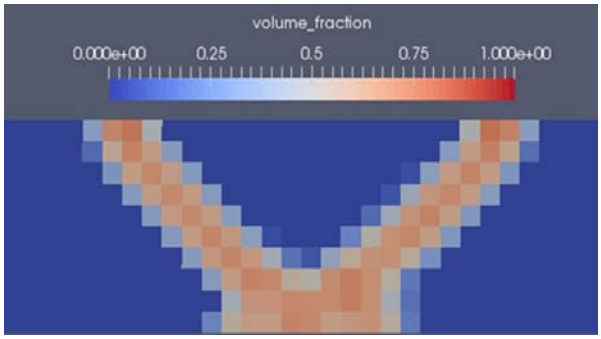

Fig. 14 Density distribution for geometry given in Fig. 13

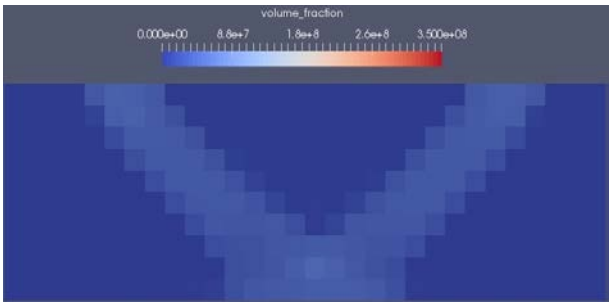

Fig. 15 Stress distribution for geometry given in Fig. 14

The density distribution (Fig. 14) varies from 0 (void) to 1 (solid). The results show a solid-like structure with angled features that meet and connect with a rectangular base region. The base is needed to support the external shear load. The inner regions of the features are light red and surrounded by dark white-colored elements. This is a product of the optimization formulation to satisfy the given objectives and constraints. Since the objective of the problem is to minimize weight, the optimization process is formulated to satisfy this objective by inserting intermediate density elements that weigh less than full-density solid elements. As seen in Eq. 7, intermediate elements also carry less stress than full-density elements, which helps in satisfying the stress constraint. The intermediate solids can be pushed toward 0–1 by increasing β in the Heaviside projection method or by artificially prescribing all elements with a density between 0 and 0.5 to 0, and prescribing all elements with a density between 0.1 and 1 to 1 during postprocessing. Figure 15 shows the stress distribution. The von Mises stress in every element is less than the prescribed stress constraint.

Table 1 shows what happens to cycles-to-failure[19] as weight is reduced. Cycles-to-failure reduces by almost 100% as weight is drastically reduced. This highlights the need to constrain cycles-to-failure as weight is reduced. The cycles-to-failure calculation is a rough estimate because the density distribution is composed of intermediate elements. Making the solution fully solid would result in a better estimate of cycles-to-failure.

Table 1 Weight vs. cycles-to-failure comparison for cantilever in shear

	Initial	**Final**	**Reduction (%)**
Weight	300	86	71
Cycles-to-failure	8×10^{14}	3×10^{12}	99.6

7.2 MMB

A second example that further demonstrates lightweighting and fatigue life is the 2-D MMB beam. The initial distribution of φ is uniform at 99%. The gradient-based optimization process used to solve these problems is "fmincon". The derivatives were provided to fmincon following the formulation in Holmberg et al.[17] Instead of distributing the load across several nodes, the method of element exclusion suggested by Holmberg[17] for reducing stress near the point of application was implemented. The density and stress distribution plots are given in Figs. 17 and 18, respectively. The density plot shows regions of full, intermediate, and void elements. The stress distribution plot shows that the maximum von Mises stress is near the application of the point load. However, the von Mises stress has not been exceeded. As in Table 1, Table 2 also shows the penalty on cycles-to-failure as weight is reduced.

Table 2 Weight vs. cycles-to-failure comparison for MMB

	Initial	Final	Reduction (%)
Weight	300	134	55
Cycles-to-failure	4×10^4	1×10^4	75

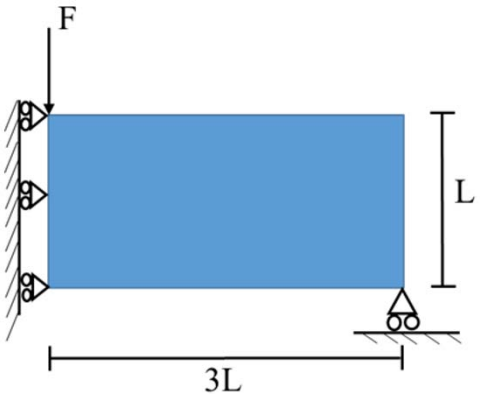

Fig. 16 Initial MMB, half-symmetry

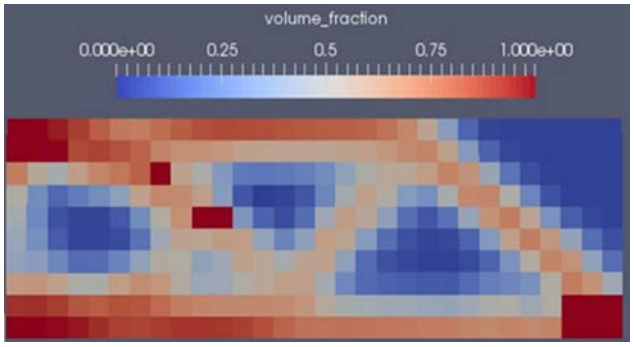

Fig. 17 Density distribution for half-symmetry MMB

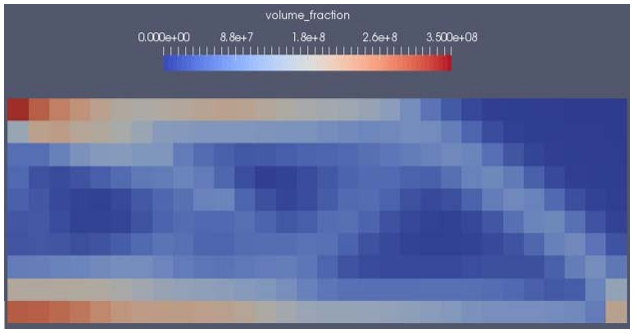

Fig. 18 Stress distribution for half-symmetry MMB

8. Summary

This report documents current progress made toward developing a methodology for AM structures that are TO when considering fatigue. To address this topic, the research has been split into 2 separate efforts: TO for AM and TO for fatigue. The TO for AM efforts are focused on accounting for AM constraints within design: 1) removal of support material and 2) the elimination of enclosed pores. To date, the 3-D projection method produces topologies with features that do not violate the overhang constraint and are therefore self-supporting. Also, the void projection scheme produces topologies with outlets for trapped material. The TO for fatigue effort is focused on using a published methodology to design structures considering fatigue. The selected methodology is Holmberg's clustered approach.[17] The methodology was successful in producing topologies that do not violate imposed stress constraints. However, it was also shown that reducing weight penalizes fatigue life.

9. Conclusions

The methodology for developing self-supporting AM structures is currently programmed to design structures with various angles, but this report showed examples of the typical design situation of 45°. Any subsequent shape or size optimizations should account for the angular overhang constraint if the structure is to remain self-supporting. The void projection method produces orifices to release trapped material. It is currently programmed to develop orifices from the bottom up. Therefore, the structures that will likely be produced are those that will allow material to escape from the bottom. It may be useful to implement an aesthetic constraint that minimizes the size of gaping orifices that are currently being produced while maintaining structural properties such as stiffness, buckling, and eigen frequency.

In considering TO for fatigue, the current solutions were developed with no attention given to the structure's fatigue life before optimization. The result was a worsening of fatigue properties. This effect can be mitigated by first assessing the fatigue life of the initial structure, then setting the fatigue constraint to this value while reducing mass. This would ensure that mass is decreased while maintaining fatigue life. In addition to maintaining fatigue life, it is proposed that TO can also be used to improve fatigue life. This can be done be allowing mass redistribution instead of mass removal. Thus, the TO for fatigue problems can be described as follows: 1) keep mass constant and change fatigue properties or 2) keep fatigue properties constant and change mass. Addressing these problems will be the focus of future work.

10. References

1. Gao W, Zhang Y, Ramanujan D, Ramani K, Chen Y, Williams CB, Wang CC, Shin YC, Zhang S, Zavattieri PD. The status, challenges, and future of additive manufacturing in engineering. Comp Aided Des. 2015;69:65–89.
2. Qian X. Undercut and overhang angle control in topology optimization: a density gradient based integral approach. Int J Num Meth Eng.
3. Guo, X, Zhou J, Zhang W, Du Z, Liu C, Liu Y. Self-supporting structure design in additive manufacturing through explicit topology optimization. Comp Meth App Mech Eng. 2017.
4. Langelaar M. Topology optimization of 3D self-supporting structures for additive manufacturing. Add Mfg. 2016;12:60–70.
5. Langelaar M. An additive manufacturing filter for topology optimization of print-ready designs. Struct Multidiscip Opt. 2016:1–13.
6. Gaynor AT, Guest JK. Topology optimization considering overhang constraints: Eliminating sacrificial support material in additive manufacturing through design. Struct Multidiscip Opt. 2016;54.5:1157–1172.
7. Mirzendehdel AM, Krishnan S. Support structure constrained topology optimization for additive manufacturing. Comp Aided Des. 2016;54.5:1–13.
8. Li Q, Chen W, Liu S, Tong L. Structural topology optimization considering connectivity constraint. Struct Multidiscip Opt. 2016;54(4):971–984.
9. Wu J, Wang CC, Zhang X, Westermann R. Self-supporting rhombic infill structures for additive manufacturing. Comp Aided Des. 2016;80:32–42.
10. Fernandez-Vicente M, Canyada M, Conejero A. Identifying limitations for design for manufacturing with desktop FFF 3D printers. Int J Rapid Mfg. 2015;5.1:116–128.
11. Papadrakakis M, Papadopoulos V, Stefanou G, Plevris V. Topology optimization for additive manufacturing with controllable support structure costs.
12. Guest JK, Prevost JH, Belytschko T. Achieving minimum length scale in topology optimization using nodal design variables and projection functions. Int J Num Meth Eng 2004;61.2:238–254.
13. Bendsoe M. Optimal shape design as a material distribution problem. Struct Opt. 2001;1(4):193–202.

14. Stolpe M, Svanberg K. An alternative interpolation scheme for minimum compliance topology optimization. Struct Multidiscip Opt. 2001;22(2):116–124.

15. Zhou M, Rozvany G. The COC algorithm, part II: topological, geometrical and generalized shape optimization. Comp Meth Appl Mech Eng. 1991;89(1–3):309–336.

16. Guest JK. Optimizing the layout of discrete objects in structures and materials: a projection-based topology optimization approach. Comp Meth Appl Mech Eng. 2015;283:330–351.

17. Holmberg E, Torstenfelt B, Klarbring A. Stress constrained topology optimization. Struct Multidiscip Opt. 2013;48.1:33–47.

18. Matlab. R2016a. 2016. [accessed June 2017] https://www.mathworks.com/products/matlab.html.

19. Schijve J. Fatigue of structures and materials. Dordrecht (NL): Kluwer Academic; 2001.

1 (PDF) DEFENSE TECHNICAL INFORMATION CTR DTIC OCA

2 (PDF) DIRECTOR US ARMY RSRCH LAB RDRL CIO L IMAL HRA MAIL & RECORDS MGMT

1 (PDF) GOVT PRINTG OFC A MALHOTRA

1 (PDF) ORAU T E JOHNSON

INTENTIONALLY LEFT BLANK.